Enhanced photoconduction of free-standing ZnO nanowire films by L-lysine treatment

Jinzhang Liu[1], Jaeku Park[1], Kyung Ho Park[2], Yeonghwan Ahn[1], Ji-Yong Park[1], Ken Ha Koh[1], and Soonil Lee[1]*

[1]Division of Energy Systems Research, Ajou University, Suwon 443-749, Korea

[2]Korea Advanced Nano Fab Center, Suwon 443-479, Korea.

*E-mail: soonil@ajou.ac.kr

Abstract

Flexible paper-like ZnO nanowire films are fabricated and the effect of L-lysine passivation of the nanowires surfaces on improving the UV photoresponse is studied. We prepare three types of nanowires with different defects contents, and find that the L-lysine treatment can suppress the oxygen-vacancy-related photoluminescence as well as enhance the UV photoconduction. The nanowires with less defects gain larger enhancement of UV photoconduction after L-lysine treatment. Reproducible UV photoresponse of the devices in humid air is obtained due to L-lysine surface passivation, ruling out the influence of water molecules in degrading the UV photocurrent.

*E-mail:soonil@ajou.ac.kr.

1.Introduction

ZnO nanowires have been demonstrated as the promising candidates for optoelectronics applications, such as field-effect transistors [1], diodes [2], light-emitting devices [3], and solar cells [4], etc. One of the important properties of ZnO nanowires is photoconduction in UV region, because of the wide band gap of ZnO (3.37 eV). The sensing properties of ZnO crystals, either to UV light or some specified gases, are known to be governed by the adsorption and desorption of gaseous molecules on the surfaces [5], therefore nanocrystals with high surface-to-volume ratios are superior in sensing applications to bulk films. In the past decade, the successful synthesis of ZnO nanostructures offered opportunities for making devices, such as field-effect transistors and sensors, by using individual nanowires/nanobelts. However, the involved lithography technique makes the fabrication process of such a tiny device complicated. So far UV photodetectors based on single or a mass of ZnO nanowires laid on rigid SiO_x/Si substrates have been studied [5-7]. Currently, flexible electronic devices are attracting attentions aiming for next generation electronics. In addition to single ZnO nanowire of which the photocurrent is low and susceptible to environmental conditions, networks of ZnO nanowires that ensure high and steady-going current signals hold the promise in flexible and high-performance sensing applications.

Previously, we reported the mass-production of ZnO nanowires by a vapor-phase reaction method and the fabrication of paper-like films using these nanowires [8]. The free-standing nanowire films can be trimmed by a blade into any shapes, and be compatibly attached to any substrates. From a practical point of view minimizing the size of a photodiode to nano scale is unnecessary for it can be excluded from integrated circuit. As for the photodetectors based on ZnO polycrystalline films the metal contacts were usually made without using any high-resolution lithography technique [9]. Analogously, the ZnO nanowire

films, on which the metal electrodes can be directly deposited, are expected to be low-cost and flexible UV detectors. In optical switch a relatively high conductivity upon light illumination and a nearly isolating status in dark are pursued. Methods for enhancing the photoconductance of ZnO nanostructures by modifying the surfaces had been carried out. For e.g., the photoconductivity was conspicuously enhanced by either decorating the nanowires surfaces with semiconducting nanoparticles, such as CdS and CdTe [10,11], or coating the nanowires with UV sensitive polymers, such as polyacrylonitrile and polystyrene sulfate [12,13]. Herein, we report the application of free-standing ZnO nanowire films as photosensing devices, and the effect of L-lysine surface passivation on enhancing of UV photoconduction. L-lysine is a monomer, differing from the UV sensitive polymers that readily form thick coatings over ZnO nanowires. Three types of nanowires with different defects contents are used in this study.

2. Experimental

Details for the large-scale synthesis of ZnO nanowires were reported previously [14]. In brief, a mixture (4 g) of ZnO and graphite powders with weight ratio of 1:1 was heated at 1150 ^{o}C in a horizontal tube furnace under atmospheric pressure in a flow of N_2 (1000 sccm) and O_2 (20-40 sccm). The cotton-like product consisting of ZnO nanowires was collected at downstream region (~50-300 ^{o}C). In this work we prepared three types of ZnO nanowries by controlling the growth condictions, O_2 flow rate and growth temperature. Type I: better-crystallinity nanowires with O_2 flow rate of 40-sccm and growth temperature of 200-300 ^{o}C; Type II: Nanowires rich of defects grown at 100-200 ^{o}C with 30-sccm O_2 flow; Type III: Nanowires rich of defects grown at 50-100 ^{o}C with 25-sccm O_2 flow. Paper-like films of the mass-produced ZnO nanowires were fabricated by a simple filtration method as illustrated in

figure 1(a). First, a suspension was prepared by ultrasonically dispersing the nanowires into isopropanol. Second, the nanowires were filtered onto a nano-porous anodic aluminium oxide (AAO) membrane. After drying, the nanowire film was detached off the membrane, and cut into straps of 2 mm wide. Metal electrodes on the straps with a gap of 5 mm were deposited by thermally evaporating Ag and Au in sequence through a shadow mask, with the thickness of 50 nm and 80 nm, respectively. We used Ag to contact the nanowires for establishing an Ohmic contact. The three types of devices, types I, II and III, owing to the different defects contents in nanowires, were used to study the UV photoresponse properties. To treat the surfaces of nanowires with L-lysine, the devices were immersed into a solution of L-lysine in ethanol with a concentration of 5 mM for 24 hours, and then were removed from the solution and rinsed with ethanol. Afterwards, the devices were dried in vacuum at room temperature. Figure 1(b) shows the scheme of photoresponse measurement of a nanowire strap under UV illumination (312 nm, 30 mW/cm^2). The UV lamp and device were set inside a glass chamber in which the relative humidity can be adjusted by inputting dry air through a moisture generator. A constant DC bias of 8 V was applied at the electrode, and the current was recorded with switching the UV lamp on and off. The samples with and without L-lysine treatment were characterized by using high-resolution transmission electron microscopy (HRTEM, JEM 2100F), field-emission electron scanning microscopy (FE-SEM, Hitachi S-4800) and room-temperature photoluminescence (PL, Hitachi F-7000).

3. Results and Discussion

Figure 2(a) is the optical photograph of a wrinkled ZnO nanowire film, showing the high flexibility. As aforementioned that the nanowire sheet can be cut by a blade, a simple device based on the strap-shaped nanowire film is shown in figure 2(b). The whole device is

bendable, including the Ag/Au electrode part. The noble metals evaporated onto the nanowire sheet ensure good adhesion and electrical contact. Figure 3(a) is a low-magnification FE-SEM image showing that the nanowires interlap with each other to form a felty morphology. A close-view FE-SEM image in figure 3(b) stresses the nanowires that had gone through the process of being immersed into a lysine-ethanol solution for 24 hours. These nanowires are about 20-50 nm in thickness, and have smooth surfaces indicating no erosion by lysine molecules. Furthermore, polymerization and aggregation of L-lysine around the nanowires are ruled out. The HRTEM images in figures 4(a) and 4(b) correspond to the type-II nanowires before and after L-lysine treatment, respectively. The insets are selected area electron diffraction patterns. The L-lysine surface treatment results in no observable change at the edge of the ZnO nanocrystal. This differs from the previous work of coating the nanowires by thick layers of functional polymers to enhance the photoconduction. Presumably, the L-lysine molecules sparsely reside at defects sites of the nanowire surface. Therefore, UV absorption of the thin lysine coating is negligible in PL characterization.

The PL spectra in figures 5(a), 5(b) and 5(c) were measured at identical conditions on the nanowire films of types I, II and III, respectively. The PL properties of the samples before and after L-lysine treatment are compared. For all the nanowires, the sharp peak at 379 nm and the broad visible band are assigned to the near band-edge (NBE) emission and defect-related emission of ZnO, respectively. After L-lysine treatment all the samples showed enhanced NBE UV emission together with decreased visible emission bands. For the type-I nanowires that contain less defects, the UV peak increases about 1.9 times in intensity compared with that before L-lysine treatment. In the PL spectra in figures 5(b), L-lysine treatment on the type-II nanowires induced a red-shift of ~30 nm for the visible band peak, as shifted from 525 nm to 555 nm. This indicates multiple kinds of defects were responsible for

98 the visible band, one of which was suppressed in luminescence due to L-lysine surface
99 passivation. Among the native defects in ZnO two kinds can contribute to the green emission
100 band, singly-charged oxygen vacancy (V_O^+) and oxygen antisite (O_{Zn}). According to the
101 calculated values of the defects levels in the energy band-gap of ZnO, the emission
102 wavelength corresponding to O_{Zn} is a bit larger than V_O^+ [14]. Therefore, we ascribe the red-
103 shift of the visible band to the reduction of surface V_O^+. The inset in figure 5(b) shows the PL
104 excitation (PLE) spectra corresponding to the emission at 520 nm. The PLE spectra of the
105 sample before and after L-lysine treatment reveal the strong UV absorption and minor visible
106 absorption of the nanowires despite of abundant crystal defects. The broad green band of the
107 type-III nanowires, centering at 570 nm, showed no obvious shift (figure 5(c)) upon L-lysine
108 treatment. Possibly this is due to the lack of surface oxygen vacancies.
109 Figures 6(a) and 6(b) show the UV photoconduction characteristics of the devices in dry
110 air with very low relative humidity (~2 %) before and after L-lysine treatment, respectively.
111 Before recording the photocurrent each device was exposed to UV illumination for 5 min and
112 then restored in dark for 3 min. This is to obtain stable photoresponse in the following
113 measurement because the photocurrent maximum in the first exposure to UV light could be a
114 bit higher, especially for the devices without L-lysine treatment. The curves for time-
115 dependence photocurrent in figure 6(a), measured with the UV light switched on and off
116 periodically, show fast decay of dark current and low photocurrent (<0.1 mA). However, after
117 L-lysine treatment all the samples showed enhanced photocurrent and prolonged decay of
118 dark current. Without L-lysine treatment the device-I had the lowest photocurrent, but gained
119 the largest enhancement (~27 times) of photocurrent after L-lysine treatment. The
120 photocurrent peaks of devices II and III were 5 and 12 times increased after L-lysine
121 treatment, respectively. In comparison with the type-I nanowires, the types II and III samples
122 have more native defects which might favor the conductivity. Therefore, the device-I showed

123 the smallest photocurrent both before and after L-lysine treatment. Among the L-lysine-
124 treated devices device-III showed the largest UV photocurrent as 0.49 mA, by which the
125 resistance of the nanowire film under UV illumination is calculated to be 16.3 kΩ. For device
126 I the decay time was prolonged from 7.2 s to 26.7 s due to L-lysine surface modification.
127 Here we define the decay time as the duration for the current to decay to 10% of the peak
128 value. The photocurrent rising and dark current decay behaviors of device II, before and after
129 lysine treatment, are plotted in figure 6(c) on a logarithmic scale with the current peak
130 normalized. The decay time of device-II was initially 7.0 s, but prolonged to 42.2 s after L-
131 lysine modification. Such a slow decay (within 1 min) of the L-lysine-treated device is
132 acceptable in some applications. It is noteworthy that the dark current was extremely low for
133 all the devices. As an example the current-voltage (I-V) curves of device-II are shown in
134 figure 6(d). The current values at 8 V were 0.11 nA and 0.63 nA for this device before and
135 after lysine treatment, respectively. Correspondingly the resistance of the nanowire film in
136 dark was in 10^{10} Ω scale.

137 Figure 7 shows the photocurrent spectral response at 8 V of device-II before and after
138 L-lysine treatment. The inset shows the power irradiance spectrum of a Xenon lamp used in
139 our monochrometer. Without coating L-lysine molecules the device demonstrated as a good
140 “visible blind” UV photodetector though strong visible PL was observed from the nanowires.
141 After L-lysine modification the photocurrent in both UV and visible regions are increased,
142 still the photocurrent rapidly decreases when the light wavelength above 400 nm.

143 The increase of photocurrent of the ZnO nanowires after L-lysine treatment is
144 consistent with the enhanced NBE UV emission in PL spectra (figure 5). We can assume
145 that the UV PL intensity I_{PL} is proportional to both the carrier concentration N and the
146 minority carrier lifetime τ, as $I_{ph} \propto N\tau$. The photocurrent I_{ph} through a nanowire can be

expressed as $I_{ph}=qNvA$, where q is the elementary charge, v is the carrier drift velocity, and A is the nanowire cross section. Hence the photocurrent is associated with the PL intensity $I_{ph} \propto I_{PL}$. Therefore the lysine-treatment-induced enhancement of NBE peak in PL spectrum implies the increase of UV photoconductance.

It had been reported that the adsorbed water molecules on ZnO nanowires surfaces play a role in UV photoresponse. Under steady UV illumination the photocurrent of a ZnO nanowire degrades in humid air due to the exchange of hydroxyl groups and ionic oxygen at the surface defect sites [15]. Figure 7 compares the UV photoresponse of device III with and without L-lysine treatment, measured in air with relative humidity of 40%. Though lacking of oxygen vacancies as revealed by PL spectra (figure 5(c)), the adsorbed water did cause the gradual degradation of photocurrent. Similar phenomenon was also observed from other two samples. However, for the L-lysine treated sample the photocurrent is much more stable, obviating the influence of adsorbed water molecules on UV photoresponse.

Now we discuss the role of L-lysine treatment in influencing the PL and UV photoresponse characteristics of the ZnO nanowires. Figure 9(a) shows a room-temperature PL spectrum of L-lysine powder. Corresponding to the emission peak the PL excitation spectrum is shown as an inset, indicating a light absorption peak at 335 nm (3.70 eV). L-lysine, $NH_2(CH_2)_4CH(NH2)COOH$, is a polar amino acid and prone to be positively charged due to the nitrogen-containing chemical groups located at the ultimate position of its side chains (figure 9(b)) [16]. Oxygen and L-lysine molecules would be preferentially adsorbed at the charged defect sites in ZnO nanowires surfaces. For the oxygen vacancies in ZnO it had been demonstrated that the dominant one was singly-ionized V_O^+ [17], formed by the ionization of doubly charged oxygen vacancies ($V_O^{2+} + e^- \rightarrow V_O^+$). Under UV illumination the photo-generated holes ($h\gamma \rightarrow h^+ + e^-$) combine with the electrons at V_O^+ sites to give

rise to green emission and render V_O^{2+}. The vacant site is so unstable that it combines with chemisorbed O^{2-} when the nanowire exposed to oxygen atmosphere. At one vacant site two electrons are trapped to form the bond $Zn^{2+} - O^{2-}$. Hence electrons are pinned near the surface and a low-conductive depletion layer is formed as shown in figure 9(c). Under UV light illumination the ionized oxygen were reduced by photo-generated holes and desorbed from the nanowire surface, releasing the trapped electrons that increase the photoconduction of the nanowire (figure 9(c)). After L-lysine surface modification some defect sites could be occupied by L-lysine molecules instead of oxygen (figure 9(d)). If a L-lysine molecule is adsorbed at the vacant site V_O^+, it would supply one electron, possibly from the ultimate NH_2 group, to stabilize the vacant defect. Hence at one vacant site only one electron from ZnO is trapped. This accounts for the a bit higher conductance of L-lysine treated sample in dark. Also under UV illumination the L-lysine molecules keep occupying the V_O^+ sites, charge interaction between ZnO and L-lysine molecules is possible that disables the role of V_O^+ as green recombination centre. It should be noted that desorption and adsorption processes coexisted, and some oxygen molecules kept sticking to the nanowire surface via Van der Waals bonding even under UV illumination. The UV light injected into the paper-like nanowire film is scattered by the interlapped nanowires. Hence for most nanowires the adsorbed oxygen molecules incompletely release electrons to ZnO upon UV irradiation. In the spectral photoresponse curves in figure 7, the photocurrent of lysine-treated nanowires is higher than that of bare nanowires in visible region, from which we conclude that the bonds between L-lysine molecules and V_O^+ are weaker than those of $Zn^{2+} - O^{2-}$. Therefore we deduce that at the vacant sites the L-lysine molecules are more readily to release electrons than the chemisorbed oxygen when exposed to the same-power UV light. This could be one reason for the higher UV photoconduction of the L-lysine treated samples. On the other hand,

the L-lysine molecule itself absorbs UV light with energy higher than 3.7 eV, through which the electrons can be excited to a higher energy state, leaving an unoccupied molecular orbital that resembles holes. The minimum of conduction band and the top of valence band of ZnO are at -4.2 eV and -7.6 eV, respectively. For L-lysine the HOMO (highest occupied molecular orbital) level was calculated to be at -10.39 eV [18], based on which the LUMO (lowest unoccupied molecular orbital) level is deduced to be at -6.69 eV. As seen from the energy diagram of the lysine-treated ZnO nanowire shown at the bottom of figure 9(d), the electrons of L-lysine can transfer from its LUMO level into the conduction band of ZnO, causing the increase of electron population for electric conduction. Meanwhile, holes from the valence band of ZnO can be accepted by the ground state of L-lysine, i.e., the photoexcited electrons at the HOMO level of lysine molecule jump into the valence band of ZnO, preventing the hole-electron recombination in ZnO. Therefore, under UV illumination the photoconduction of lysine-treated ZnO nanowires is enhanced. The point defect O_{Zn}, rich in types II and III nanowires, refers to an oxygen atom wrongly occupies a site on the zinc sublattice. Such a site in ZnO surface is negatively charged that adsorbs oxygen or L-lysine molecules. Among the L-lysine-treated samples device-I has the smallest UV photoconduction, which could be attributed to the smallest quantity of adsorbed L-lysine molecules due to the better crystallinity of the type-I nanowires.

Therefore, the L-lysine molecules bear two roles influencing the UV photoconduction of ZnO. One is that the small molecules resemble oxygen to capture electrons from ZnO in dark and release them under UV illumination; The other is that it acts as a UV sensitive material to assist the UV conduction of ZnO. After switching off the UV light, oxygen molecules were swiftly re-adsorbed on the nanowires surfaces, and the dark current of the bare nanowires plummeted. However, surface traps were reduced for the nanowires passivated by L-lysine. Once in dark the re-adsorbed oxygen played a partial role in decreasing the conductivity. The

220 immobile lysine molecules were not as swift as oxygen to immediately capture electrons
221 from ZnO. Also the L-lysine layer could act as a buffering media to hold charges from ZnO
222 for a while, resulting in prolonged decay time of the dark current. Nevertheless, the dark
223 current decay time of the nanowire films treated with L-lysine are comparable, or even
224 shorter, than some UV photodetectors based on single ZnO nanowires reported in references
225 [19,20].
226

227 ## 4. Conclusion.

228 In summary, we have made flexible UV photosensors based on free-standing ZnO
229 nanowire films. The mass-produced nanowires, in which the defects contents can be
230 controlled, were processed into paper-like films. Three types of nanowires with different PL
231 properties were used to make visible-blind UV photodetectors and to investigate the effect of
232 L-lysine surface treatment on improving the UV photoconduction. We found that the L-lysine
233 molecules adsorbed on ZnO nanowires surfaces suppressed the oxygen-vacancy-related PL
234 emission, and increased the NBE emission of ZnO. As a result, the UV photoconduction of
235 the nanowires was enhanced after L-lysine treatment. The enhancement showed a defect-
236 dependence, for the type-I nanowires with the lowest defects contents gained the largest
237 enhancement of ~27 times induced by L-lysine surface treatment. Those rich of defects
238 exhibited higher UV photoconduction, both before and after L-lysine treatment. The time for
239 dark current decay was prolonged after L-lysine treatment, but was within 1 minute which
240 may be adequate for some applications. The surface passivation by L-lysine led to
241 reproducible UV photoresponse in humid air, ruling out the influence of water molecules that
242 cause gradual degradation of UV photocurrent of ZnO nanowires.

243 This work was supported by Priority Research Centers Program through the National

Research Foundation of Korea (NRK) funded by the Ministry of Education, Science and Technology 2009-0094049. Financial support from The Ajou University Excellence Research Program in 2010 is also acknowledged.

References

[1] Cha S N, Jang J E, Choi Y, Amaratunga G A J, Ho G W, Welland M E, Hasko D G, Kang D -J and Kim J M 2006 *Appl. Phys. Lett*. **89** 263102

[2] Heo Y W, Tien L C, Norton D P, Pearton S J, Kang B S, Ren F and LaRoch J R 2004 *Appl. Phys. Lett*. **85** 3107

[3] Bao J, Zimmler M A, Capasso F, Wang X and Ren Z F 2006 *Nano Lett*. **6** 1979

[4] Law M, Greene L E, Johnson J C, Saykally R and Yang P 2005 *Nature Mater*. **4** 455

[5] Li Q H, Gao T, Wang Y G and Wang T H 2005 *Appl. Phys. Lett.* **86** 123117

[6] Heo Y W, Kang B S, Tien L C, Norton D P, Ren F, LaRoche J R and Pearton S J 2005 *Appl. Phys. A*. **80** 497

[7] Zheng X J, Yang B, Zhang T, Jiang C B, Mao S X, Chen Y Q and Yuan B 2009 *Appl. Phys. Lett*. **95** 221106

[8] Liu J, Ahn Y H, Park J -Y, Koh K H and Lee S 2009 *Nanotechnology* **20** 445203

[9] Zhang D H and Brodie D E 1995 *Thin Solid Films* **261** 334

[10] Fang F, Zhao D X, Li B H, Zhang Z, Zhang J Y and Shen D Z 2008 *Appl. Phys. Lett*. **93** 233115

[11] Aga Jr R S, Jowhar D, Veda A, Pan Z, Collins W E, Mu R, Singer K D and Shen J 2007 *Appl. Phys. Lett*. **91** 232108

[12] He J H, Lin Y H, McConney M E, Tsukruk V V, Wang Z L and Bao G 2007 *J. Appl.*

Phys. **102** 084303

[13] Lao C S, Park M C, Kuang Q, Deng Y, Sood A K, Polla D L and Wang Z L 2007 *J. Am. Chem. Soc.* **129** 12096

[14] Liu J, Lee S, Ahn Y H, Park J -Y and Koh K H 2009 *J. Phys. D: Appl. Phys*. **42** 095401

[15] Ahn S -E, Ji H J, Kim K, Kim G T, Bae C H, Park S M, Kim Y K and Ha J S 2007 *Appl. Phys. Lett.* **90** 153106

[16] Hernández B, Pflüger F, Derbel N, Coninck J D and Ghomi M 2010 *J. Phys. Chem. B* **114** 1077

[17] Vanheusden K, Warren W L, Seager C H, Tallant D R, Voigt J A and Gnade B E 1996 *J. Appl. Phys*. **79** 7983

[18] Lopachin R M, Gavin T, Petersen D R and Barber D S 2009 *Chem. Res. Toxicol*. **22** 1499

[19] Heo Y W, Kang B S, Tien L C, Norton D P, Ren F, La Roche J R and Pearton S J 2005 *Appl. Phys. A* **80** 497

[20] Soci C, Zhang A, Xiang B, Dayeh S A, Aplin D P R, Park J, Bao X Y, Lo Y H and D Wang 2007 *Nano Lett*. **7** 1003

Figure Captions

Figure 1. (a) Illustration of the process to make a ZnO nanowire film. (b) Schematic of the UV photoresponse measurement.

Figure 2. Optical photographs of (a) a wrinkled ZnO nanoewire film and (b) a strap-shaped photodetector based on the nanowire film.

Figure 3. (a) FE-SEM image of a ZnO nanowire film. (b) High-magnification FE-SEM image of the ZnO nanowires with surfaces passivated by L-lysine molecules.

Figure 4. (a) and (b) HRTEM images for the ZnO nanowires before and after L-lysine treatment, respectively. The insets are the corresponding SAED patterns. No observable lysine coating over the surface in (b).

Figure 5. Room-temperature PL spectra of the ZnO nanowire films before (solid line) and after (dashed line) L-lysine treatment. (a) type-I nanowires. (b) Type-II nanowires. The inset shows the PLE spectrum for the visible band. (c) Type-III nanowires.

Figure 6. (a) Time-resolved photocurrent of three devices before L-lysine treatment, at 8 V in response to a UV lamp that is switched on and off periodically. (b) UV photoresponse characteristics of the three devices after L-lysine treatment. (c) UV response of device II with the photocurrent normalized. The current is on a logarithmic scale. (d) I-V curves of device II in dark, before and after L-lysine treatment.

Figure 7. Spectral photoresponse of device II, with and without L-lysine treatment. The inset is the spectrum of Xenon lamp.

Figure 8. Photoresponse of device-III, before and after L-lysine treatment, measured in humid air.

Figure 9. (a) PL spectrum of L-lysine powder. Inset is the corresponding PLE spectrum. (b) Molecular structure of L-lysine. (c) and (d) Illustrations for the photoresponse mechanisms of bare and L-lysine passivated ZnO nanowires, respectively. The color gradient in the cross-section of ZnO nanowire indicates a depletion layer near the surface.

Figures and Captions

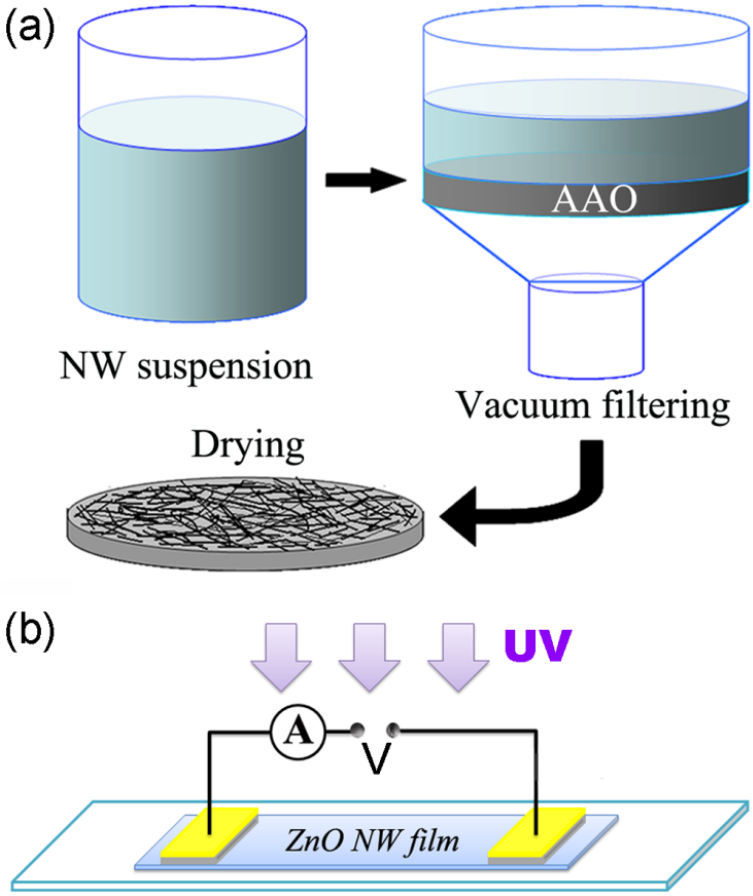

Figure 1. (a) Illustration of the process to make a ZnO nanowire film. (b) Scheme of the UV photoresponse measurement on a device.

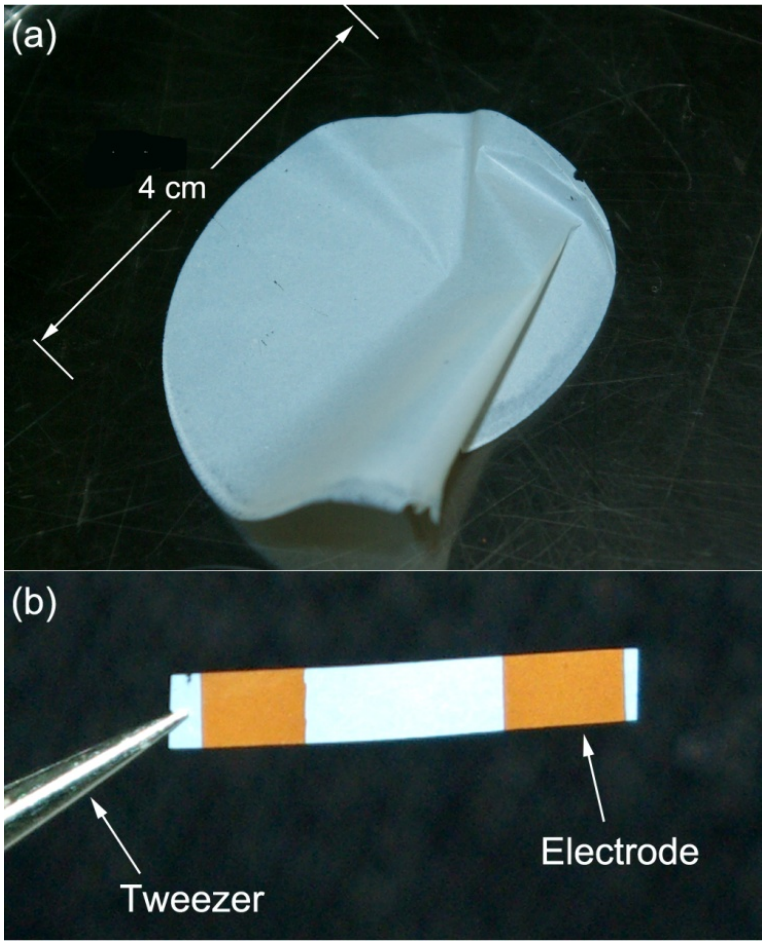

335

336

337 **Figure 2**. Optical photographs of (a) a wrinkled ZnO nanoewire film and (b) a strap-shaped

338 photodetector based on the nanowire film.

339

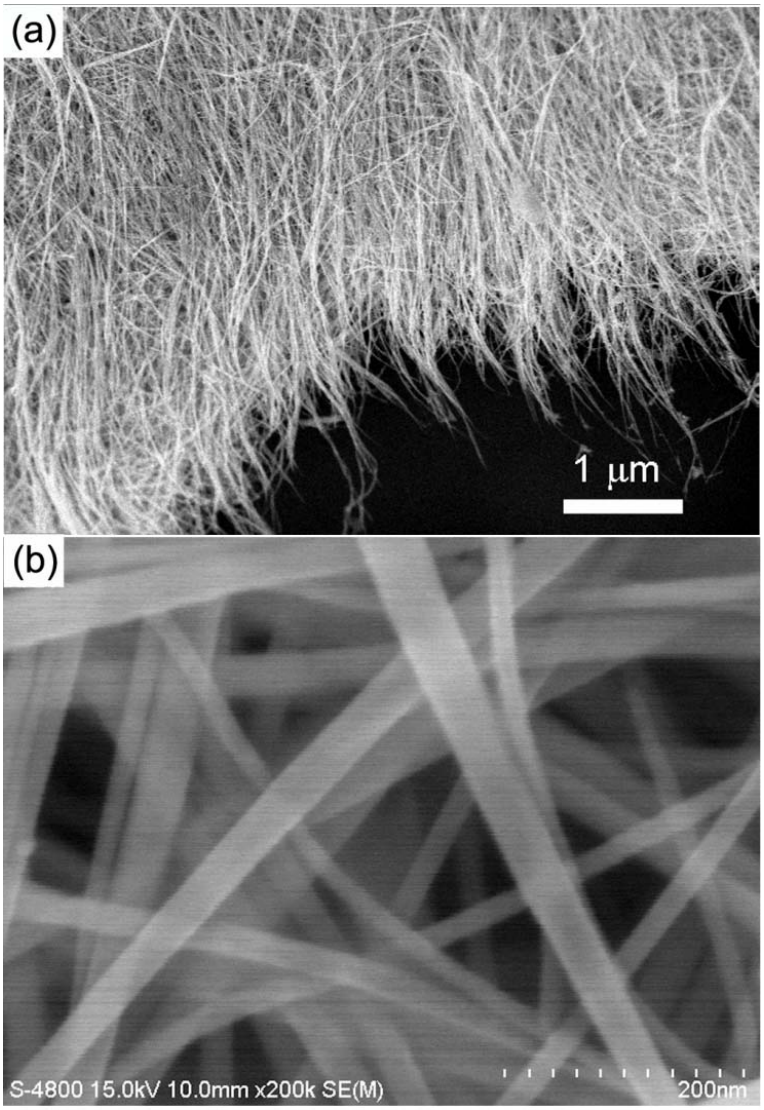

Figure 3. (a) FE-SEM image of a ZnO nanowire film. (b) High-magnification FE-SEM image of the ZnO nanowires with surfaces passivated by L-lysine molecules.

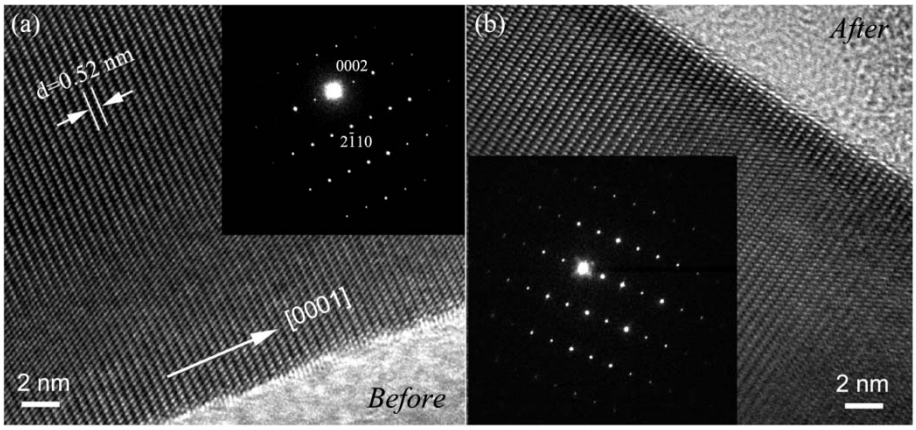

Figure 4. (a) and (b) HRTEM images for the ZnO nanowires before and after L-lysine treatment, respectively. The insets are the corresponding SAED patterns. No observable lysine coating over the surface in (b).

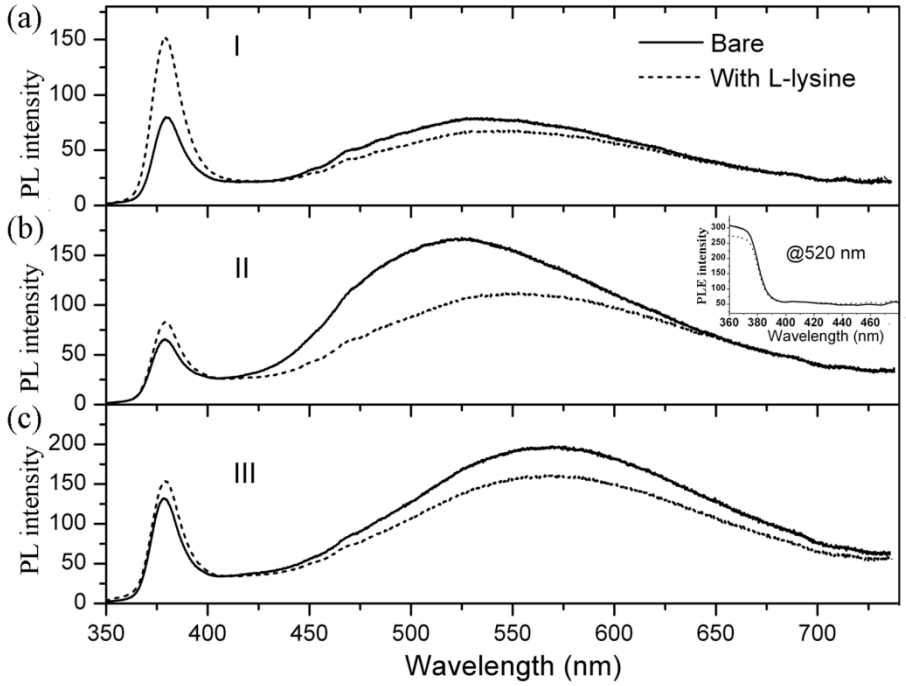

Figure 5. Room-temperature PL spectra of the ZnO nanowire films before (solid line) and after (dashed line) L-lysine treatment. (a) type-I nanowires. (b) Type-II nanowires. The inset shows the PLE spectrum. (c) Type-III nanowires.

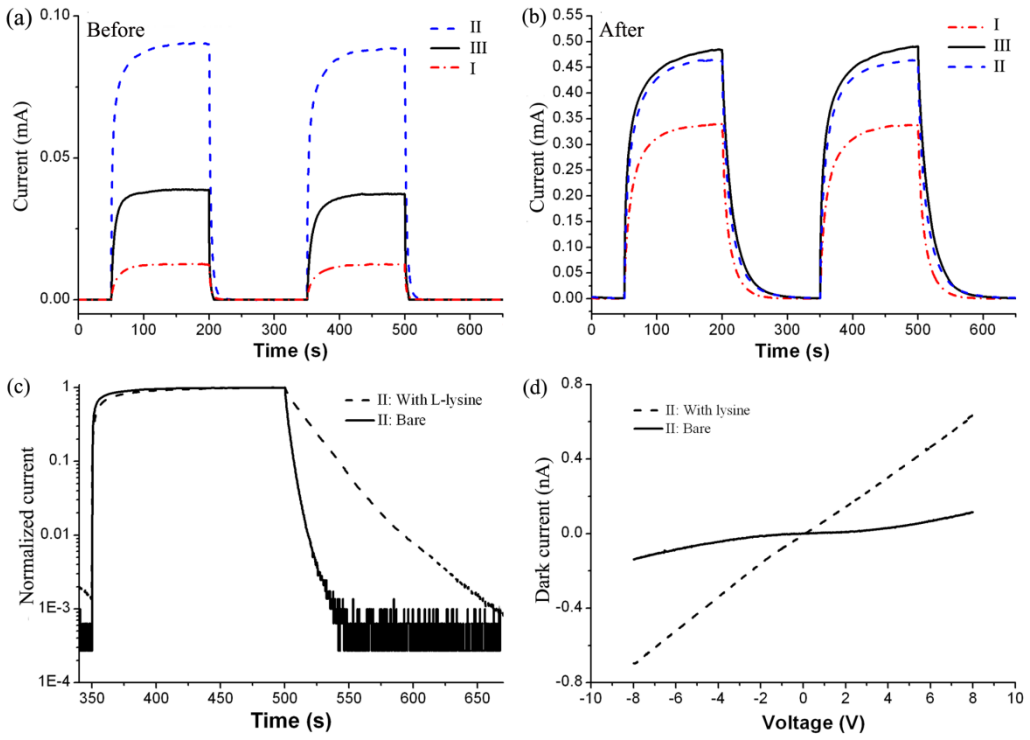

Figure 6. (a) Time-resolved photocurrent of three devices before L-lysine treatment, at 8 V in response to a UV lamp that is switched on and off periodically. (b) UV photoresponse characteristics of the three devices after L-lysine treatment. (c) UV response of device II with the photocurrent normalized. The current is on a logarithmic scale. (d) I-V curves of device II in dark, before and after L-lysine treatment.

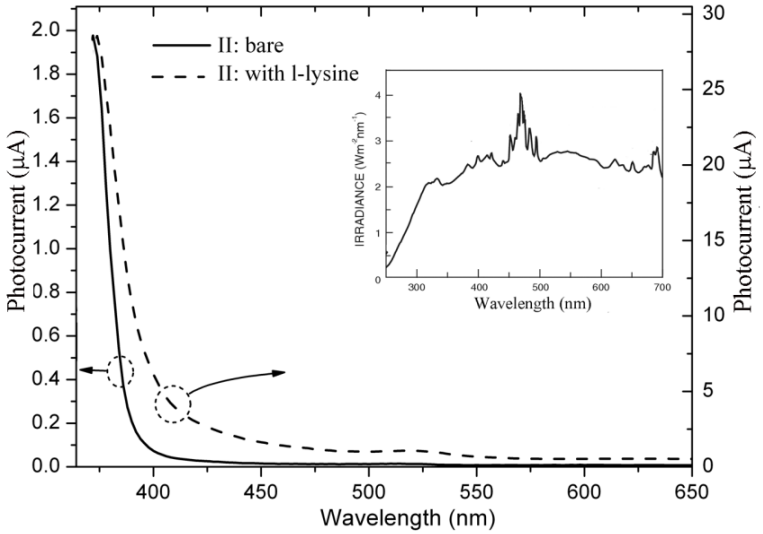

Figure 7. Spectral photoresponse of device II, with and without L-lysine treatment. The inset is the spectrum of Xenon lamp.

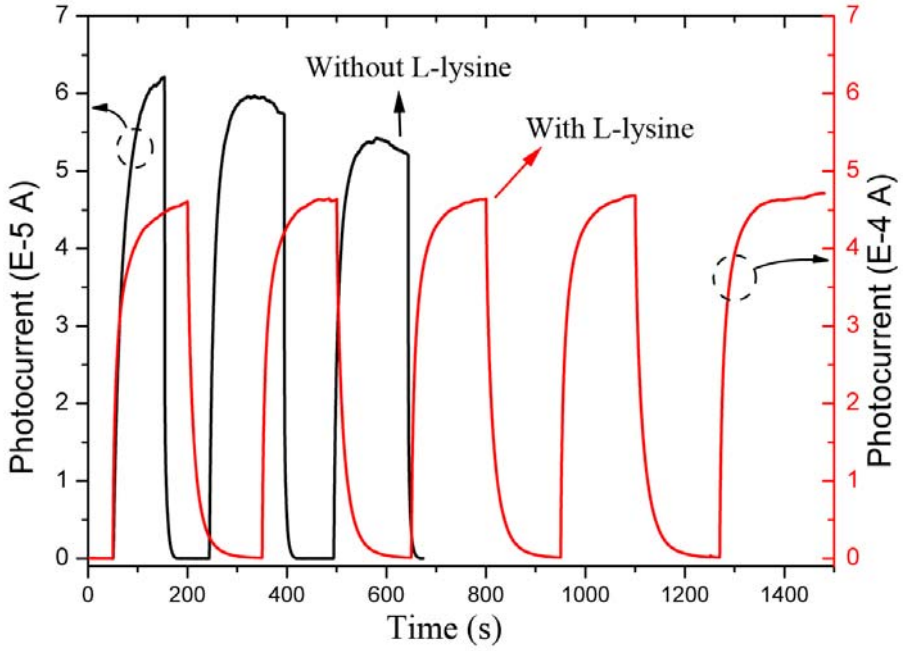

Figure 8. Photoresponse of device-III, before and after L-lysine treatment, measured in humid air.

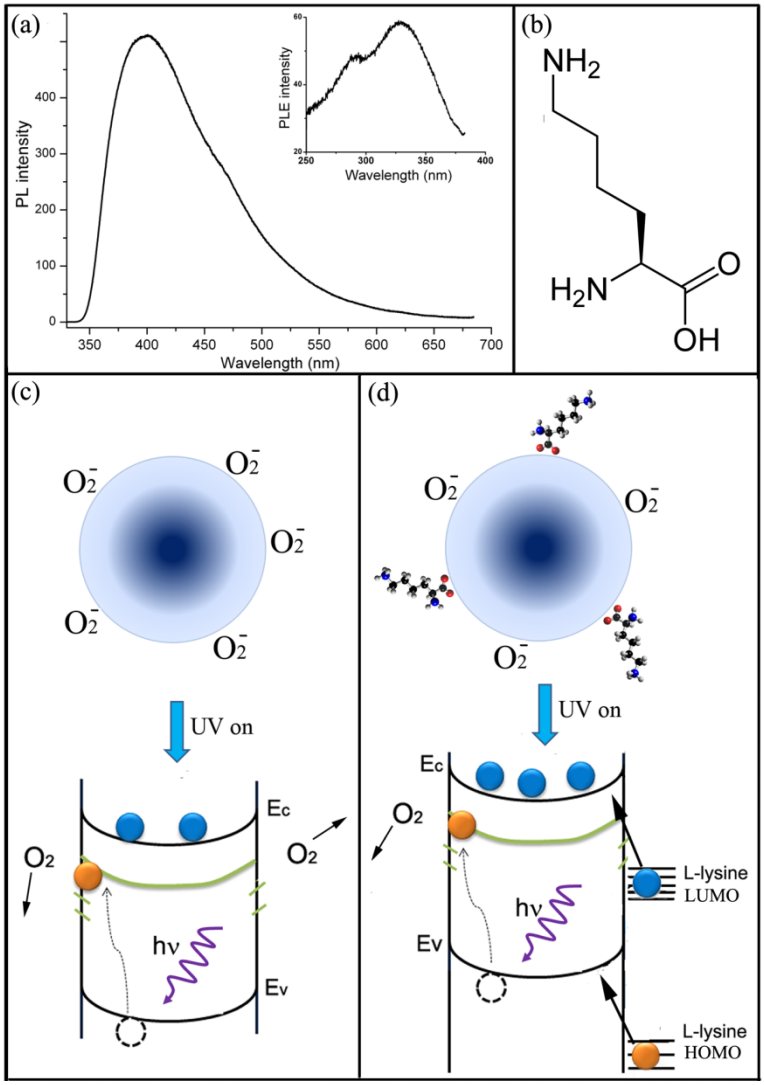

Figure 9. (a) PL spectrum of L-lysine powder. Inset is the corresponding PLE spectrum. (b) Molecular structure of L-lysine. (c) and (d) Illustrations for the photoresponse mechanisms of bare and L-lysine passivated ZnO nanowires, respectively. The color gradient in the cross-section of ZnO nanowire indicates a depletion layer near the surface.